SAND2017-6449C

Use of the Conformal Decomposition Finite Element Method for Coupled Electrochemical-Mechanical Simulations of Lithium-Ion Battery Electrodes

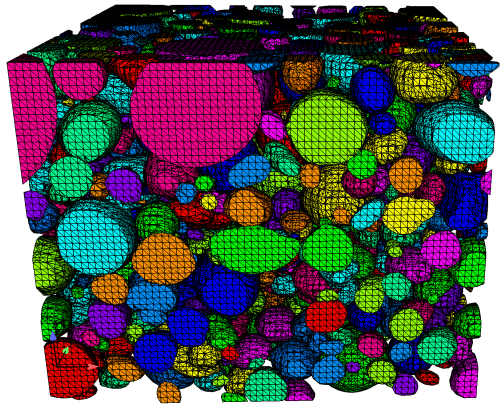

Scott A. Roberts, Hector Mendoza, Bradley Trembacki, Mark Ferraro, Victor Brunini, David Noble

Thermal/Fluid Component Sciences
Engineering Sciences Center
Sandia National Laboratories, Albuquerque, NM

July 18, 2017
14th U.S. National Congress on Computational Mechanics
MS804: Complex Multi-Physics Coupling Techniques: Advances and Applications

Sandia National Laboratories is a multi-program laboratory managed and operated by Sandia Corporation, a wholly owned subsidiary of Lockheed Martin Corporation, for the U.S. Department of Energy's National Nuclear Security Administration under contract DE-AC04-94AL85000.

Mechanics of capacity fade in lithium-ion batteries

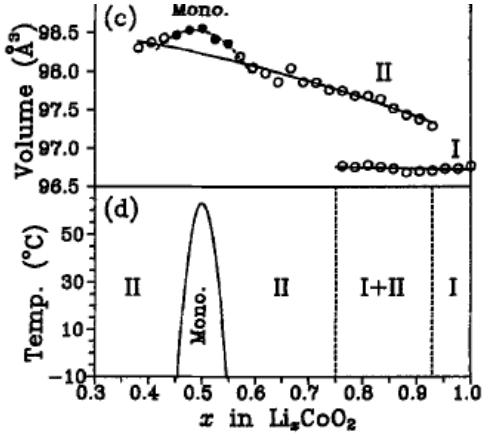

Li changes lead to strain. Reimers and Dahn (1992)

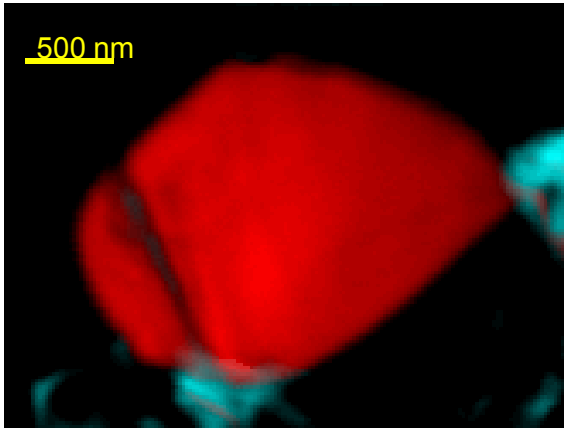

Un-cycled $LiCoO_2$

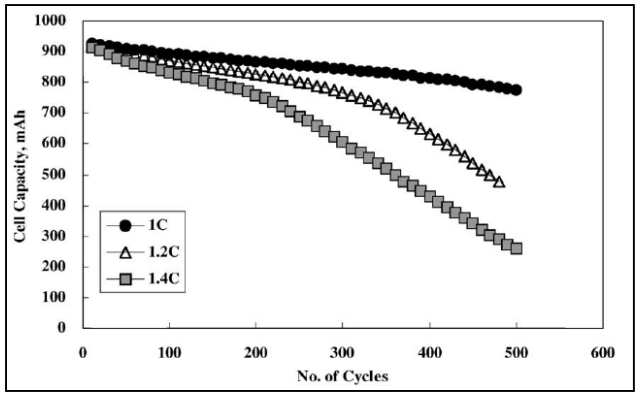

Capacity fades as batteries are cycled

- Faster discharge rates cause greater reductions in cell capacity

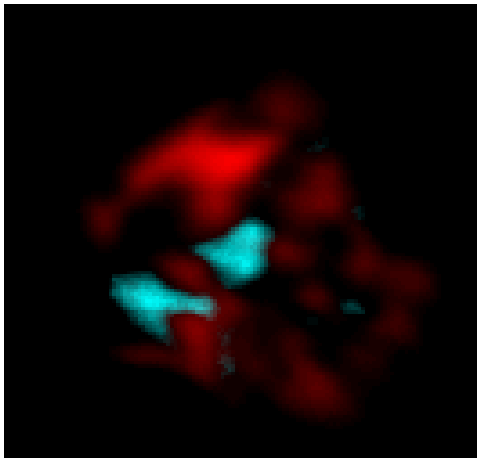

$LiCoO_2$ after 400 Cycles

Mechanical degradation leads to capacity fade

Hypothesis: Capacity fade occurs due to structural damage to electrode network

Choi et al (2002); Wilson et al (2011); Images courtesy of Farid El Gabaly, Sandia National Labs

Previous research into mechanical degradation

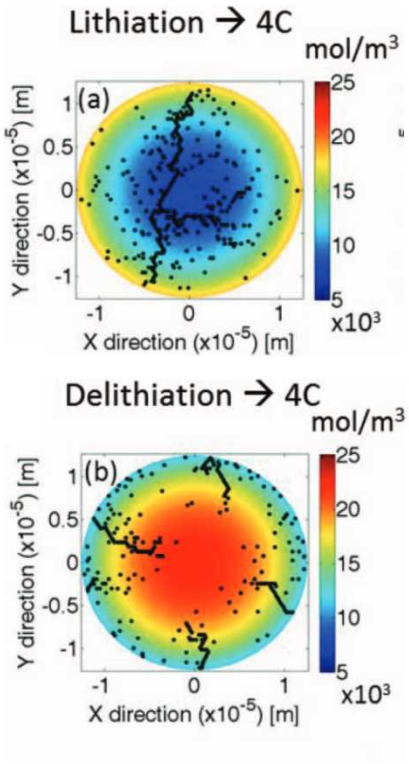

Lithiation-induced particle fracture. Barai and Mukherjee (2013)

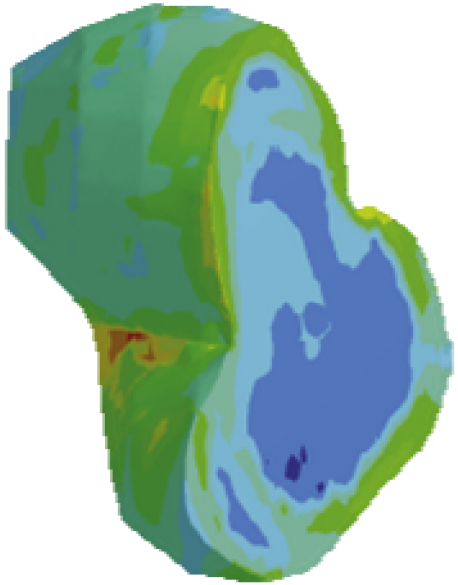

Lithiation-induced swelling, stress concentrators. Malave et al (2014)

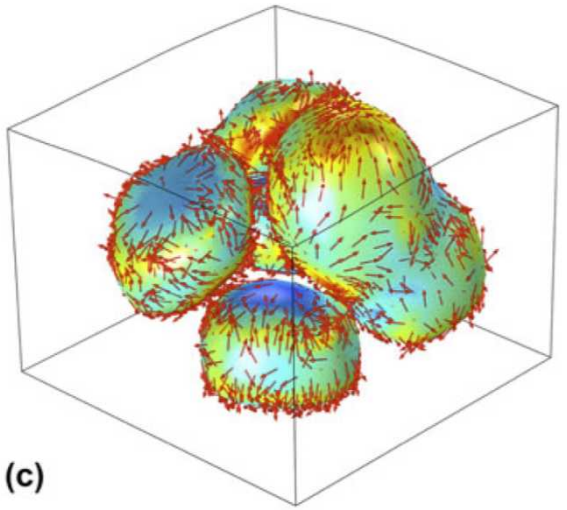

Mean stress contours and Li flux in SnO anodes, swelling 250%. Xu et al. (2016)

Microstructural details can have a significant effect on particle network degradation

Outline

- Imaging and reconstruction of cathode microstructures
  - Conformal Decomposition Finite Element Method (CDFEM)
  - Verification: Mesh and domain size requirements
  - Representing the active binder
- Effective electrode properties
- Coupled electrochemical-mechanical simulations
- Summary and a look forward

Computational approach: CDFEM

- Sierra/Aria (Sandia's Multiphysics Finite Element Method code)
  - Allows segregated or monolithic solves
- Meshing complex microstructure very difficult
  - Conformal mesh required for interface/surface physics
- Conformal Decomposition Finite Element Method (CDFEM)
  - Begins with a regular or arbitrary background mesh
  - Decomposes mesh along interfaces (STL microstructure description)
  - Additional features:
    - Adaptive mesh refinement for detailed interface representation
    - Support for multiple phases (required for binder)
    - Arbitration of overlapping
    - Guaranteed mesh quality (coming soon!)

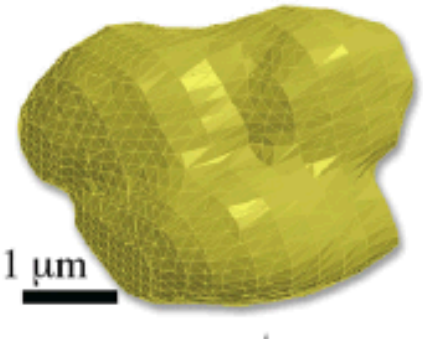

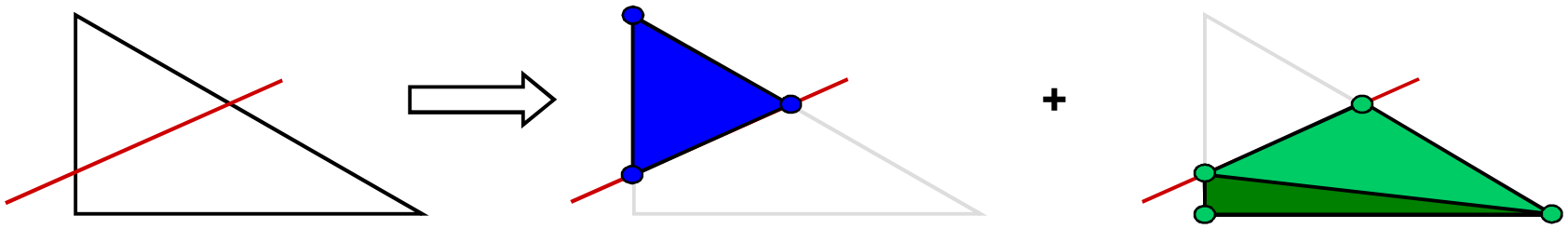

CDFEM as a method for automated meshing of complex shapes

Imaging battery cathodes

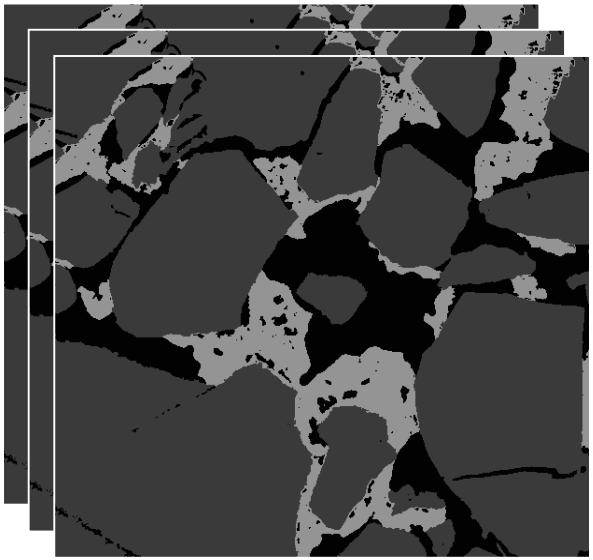

LCO with binder from FIB/SEM,
35 nm resolution,
20 µm domain.
Hutzenlaub et al (2012)

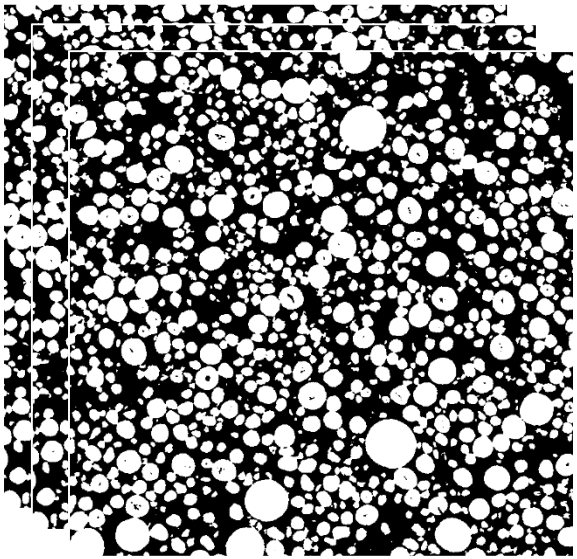

NMC from XRCT,
370 nm resolution,
757 µm domain.
Ebner et al (2013)

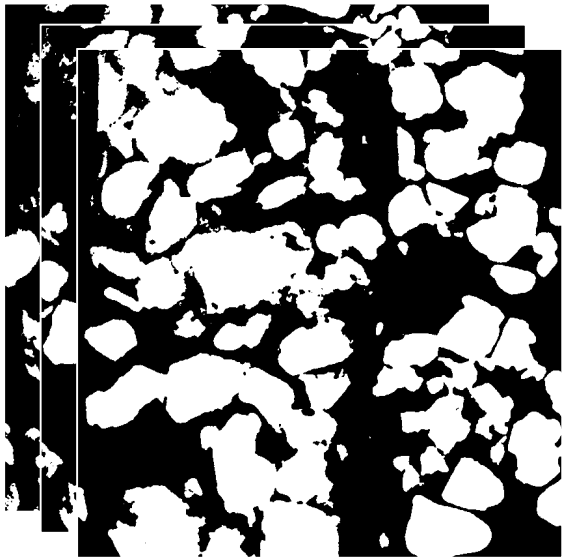

LCO from XRCT,
64 nm resolution,
22 µm domain.
Yan et al (2012)

Imaging reveals complex networks; binder can be difficult to detect at scale

CDFEM for mesh generation

- Binarize and label individual particles, surface mesh to STL files (Avizo software)

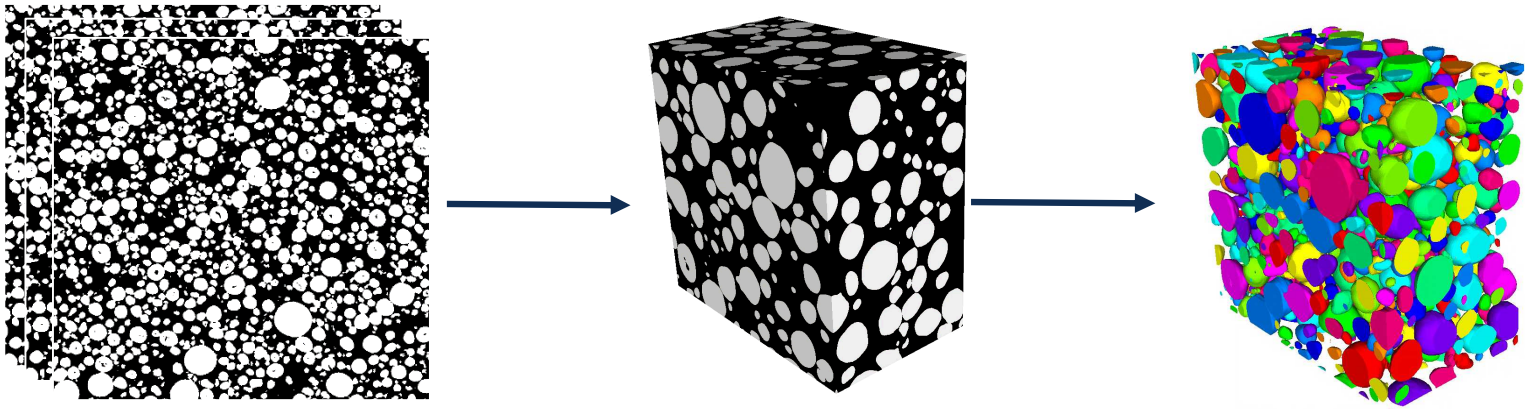

Ebner (2013)

- CDFEM creates level-set field, cuts background mesh to create conformal mesh

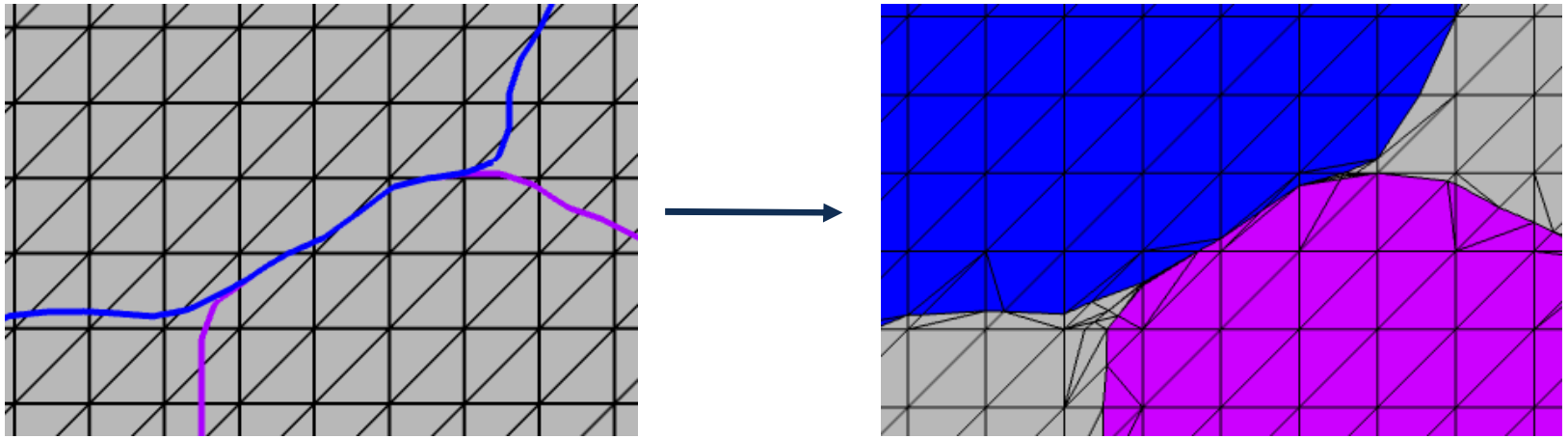

Efficient algorithm to go from images to conformal, multi-phase mesh

CDFEM for mesh generation

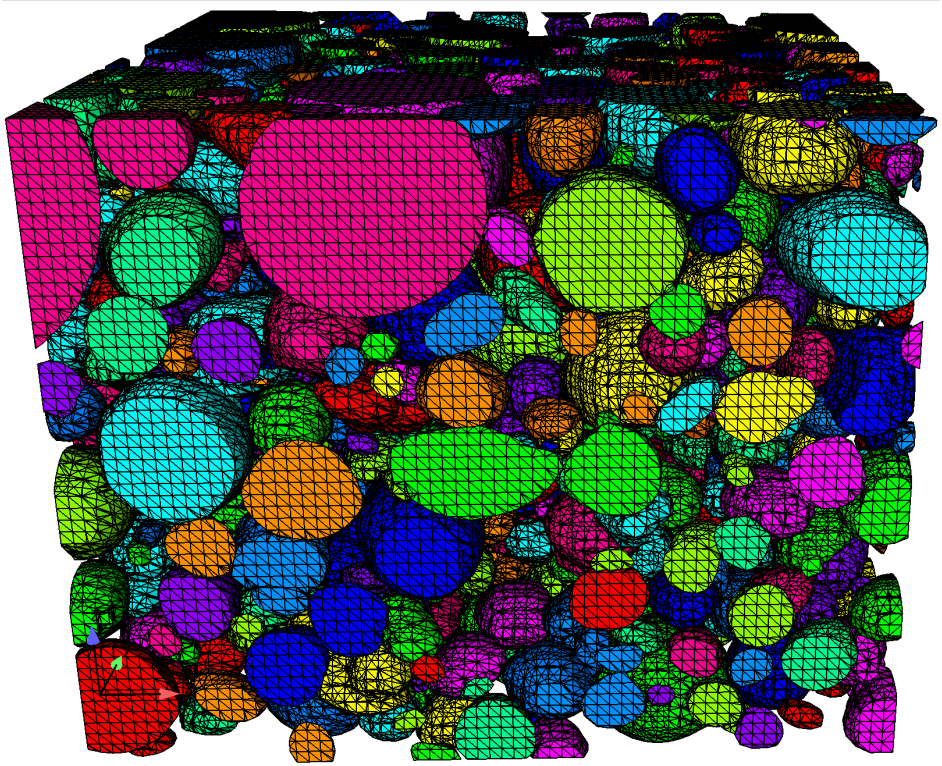

Particles

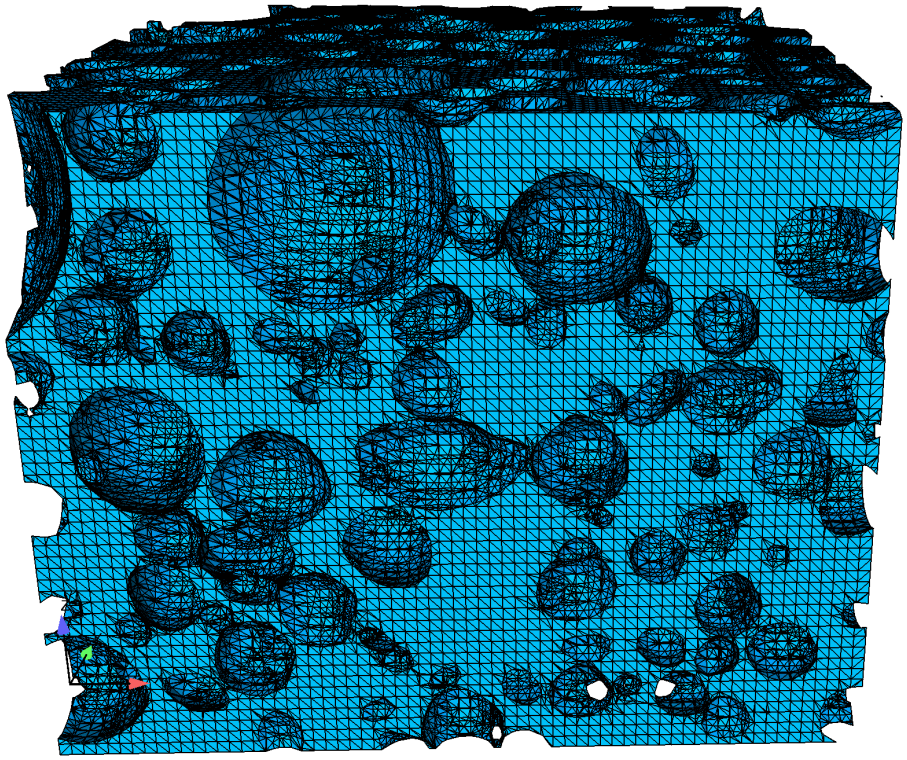

Electrolyte

Efficient algorithm to go from images to conformal, multi-phase mesh

Multiple level-set fields for particle resolution

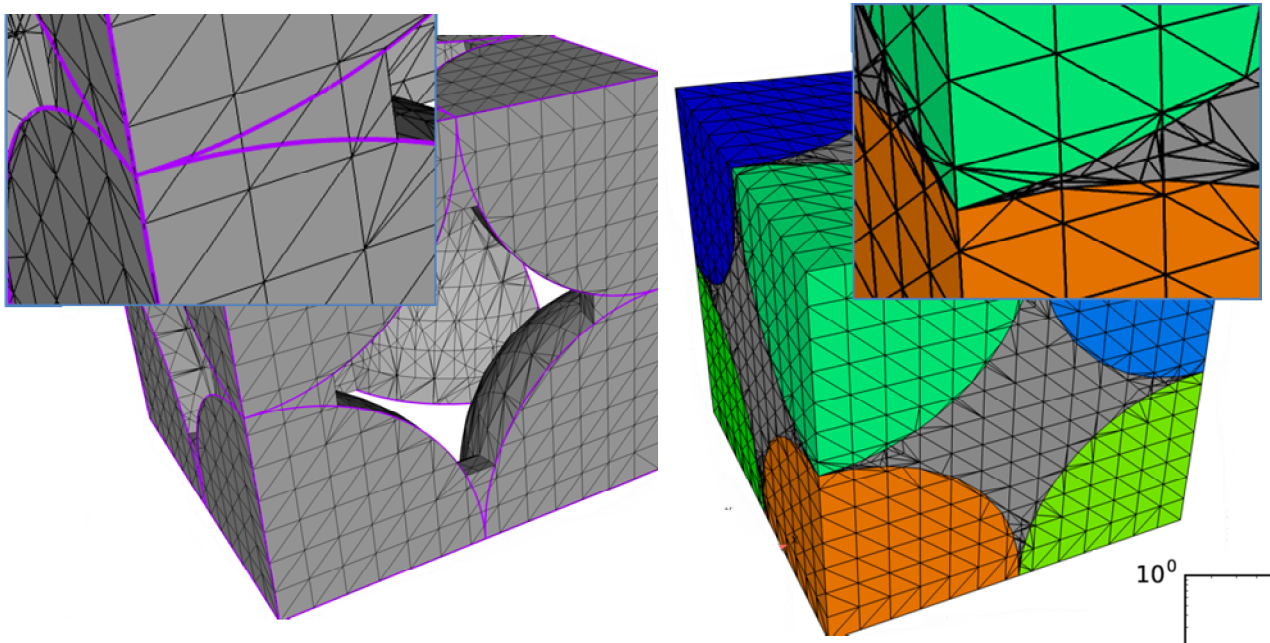

- Single level-set field (upper-left) introduces significant errors in high-curvature regions
- Labeled particles and multiple level-set fields (upper-right):
  - Enable additional physics (anisotropic expansion, contact)
  - Improve mesh convergence (right)

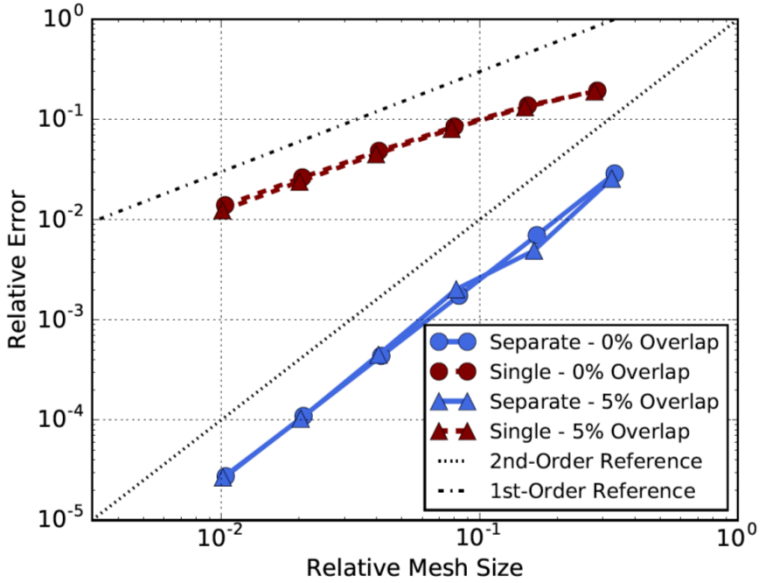

Labeled particles critical for accuracy, physics

Mesh convergence: Simple sphere geometry

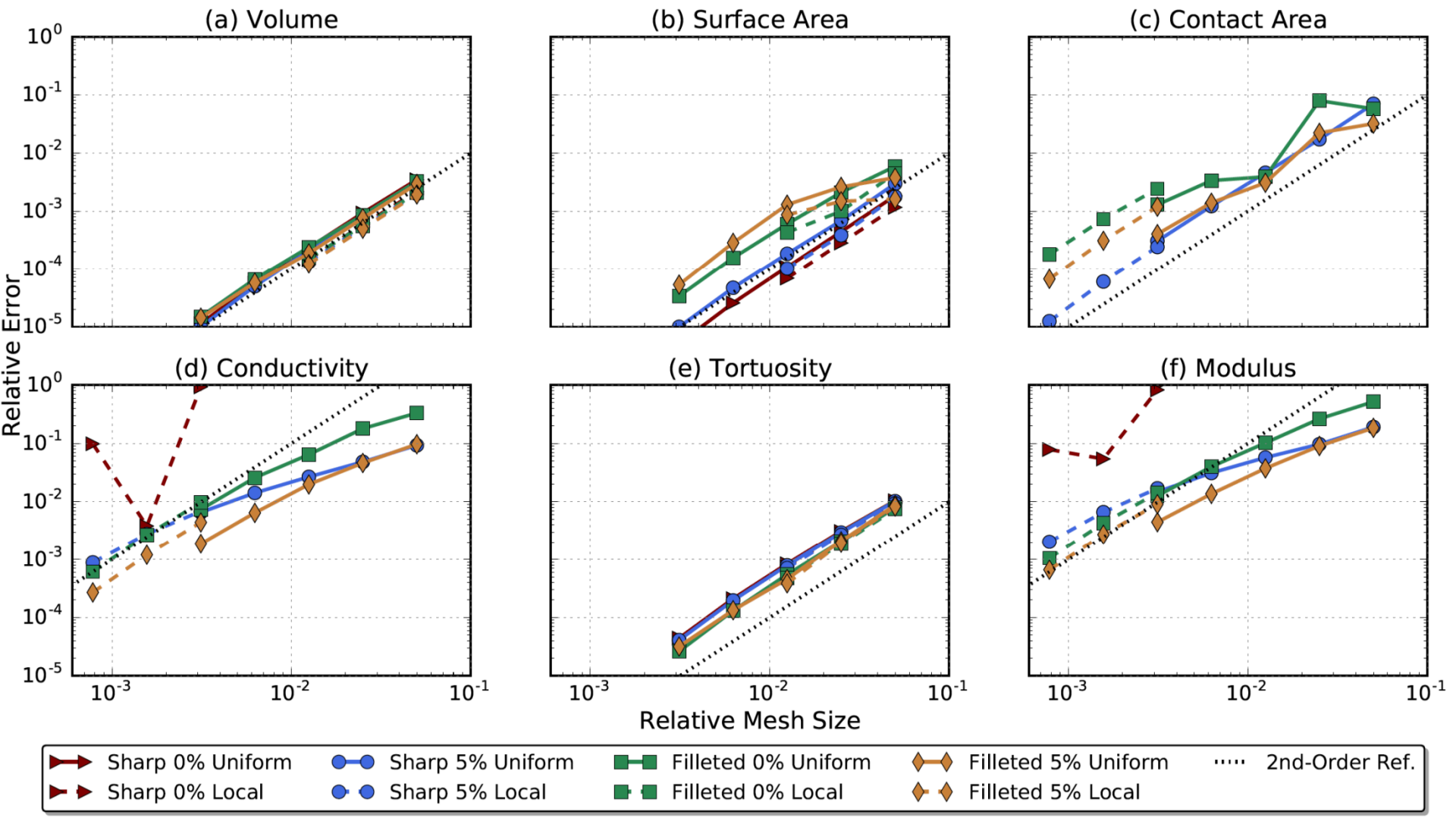

Second-order convergence – difficult physics

Mesh convergence: Image-based microstructure

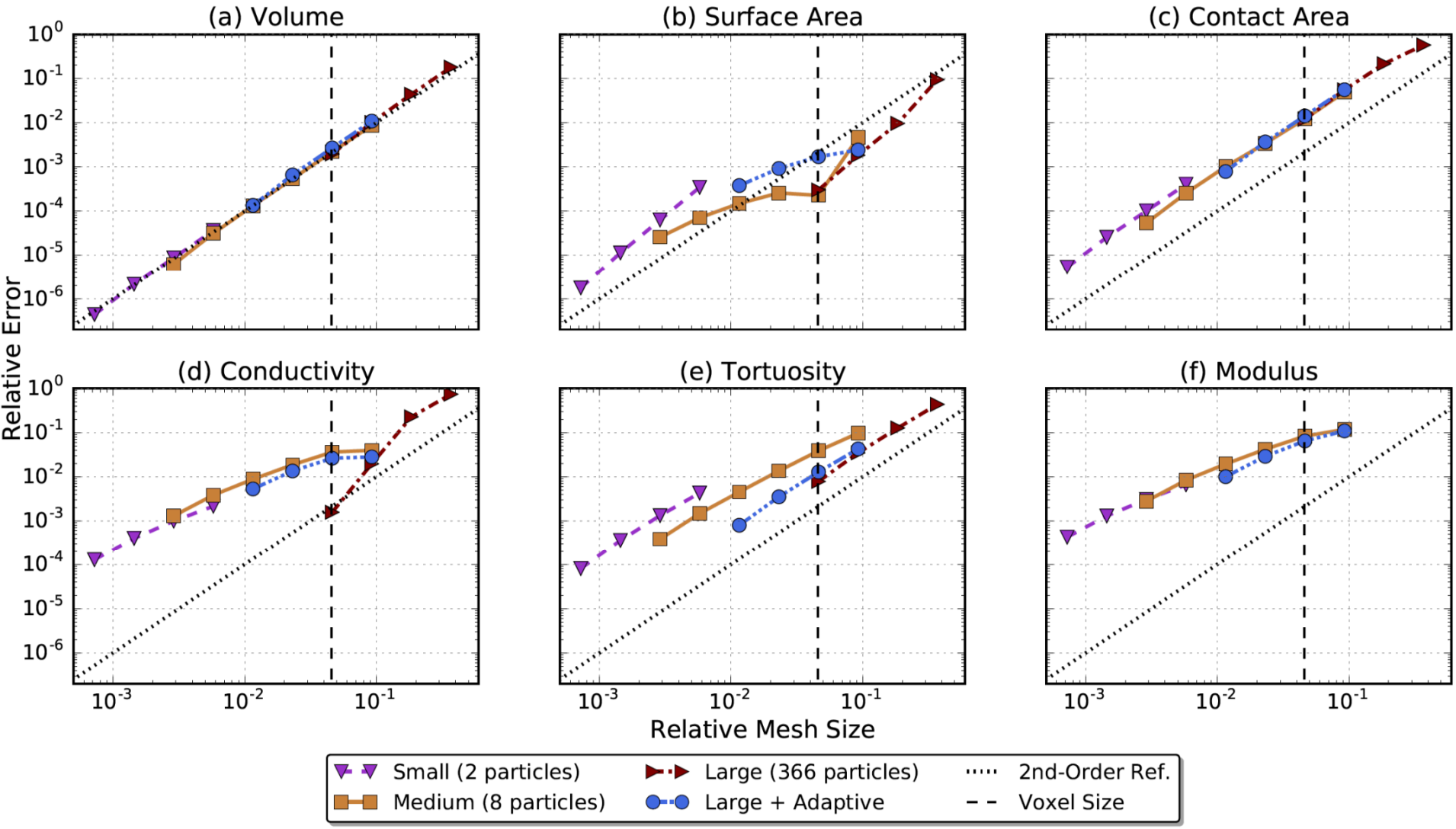

Image-based microstructure converges; adaptive refinement helps

Impact of adaptive mesh refinement (AMR)

- Biggest impact of AMR for many elements
- Up to an order-of-magnitude reduction in element counts for same relative error

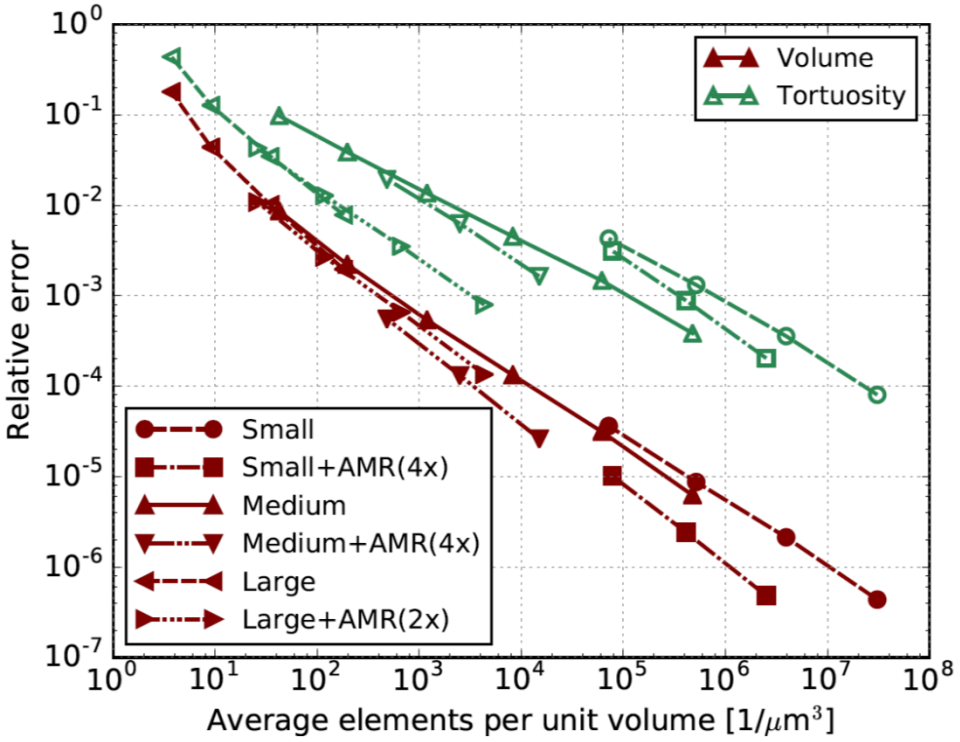

AMR can drastically lower element counts

Domain size / RVE requirements

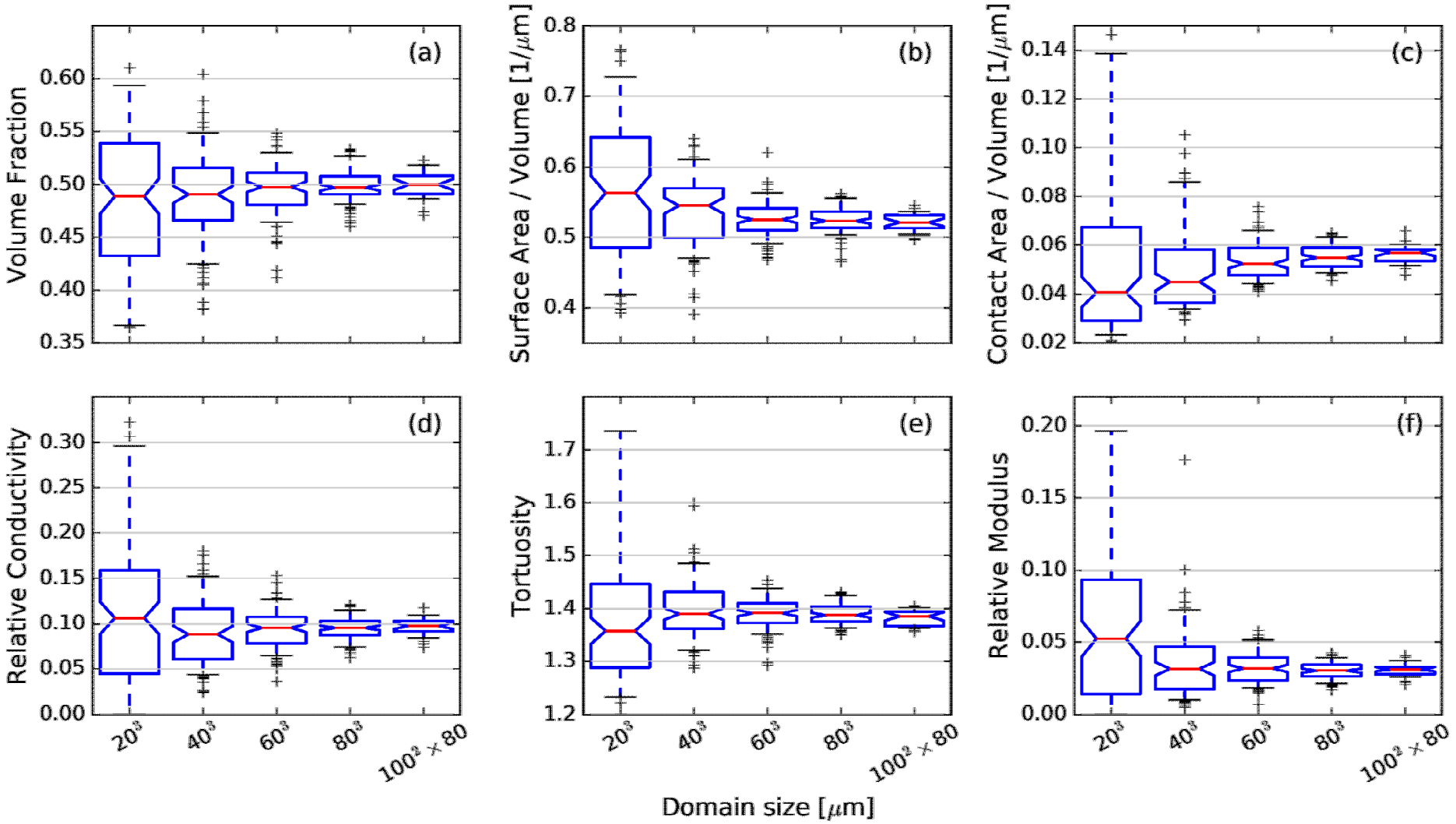

Investing in larger domain / RVE more important than refined mesh

What about the active (conductive) binder?

- Resolving the location of active binder (PVDF + CB) is much more difficult than particle image segmentation.
- Binder is often neglected, assuming non-active void space is entirely electrolyte.
- Limited imaging results can hint at binder location

CB/PVDF wt %	NMC/AB Volume Ratio
2-2 wt%	9.62
3-3 wt%	6.23
4-4 wt%	4.61
5-5 wt%	3.61

CB = carbon black
AB = active binder = PVDF + CB

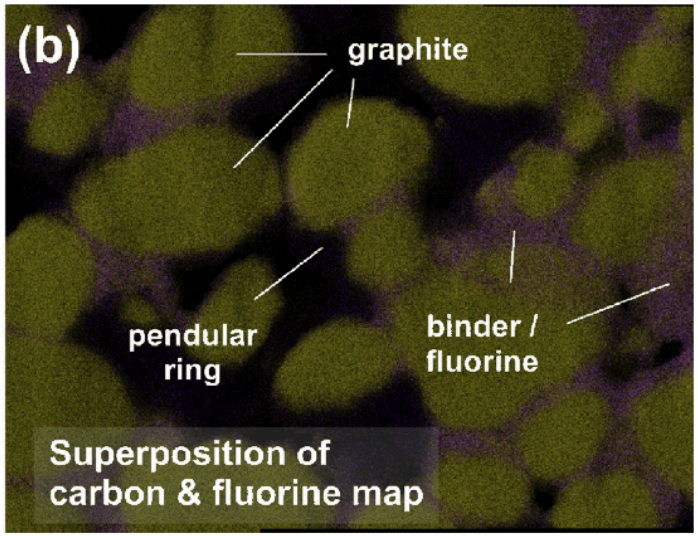

Jaiser et al. (2017)

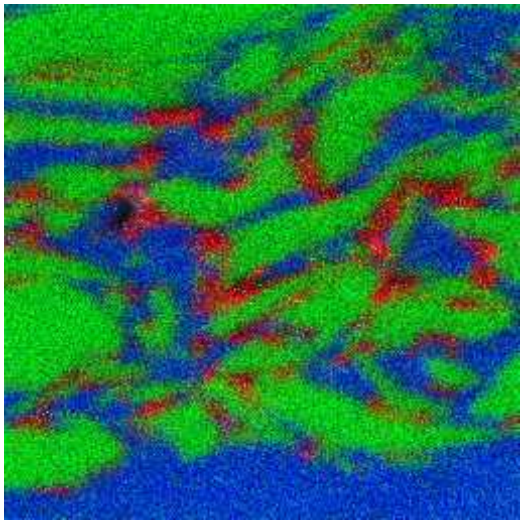

TOF-SIMS for graphite anode (Tony Ohlhausen)

Red: PVDF
Green: Carbon
Blue: Epoxy (Voids)

How are electrode-scale properties affected by inclusion of binder?

Modeling the active binder

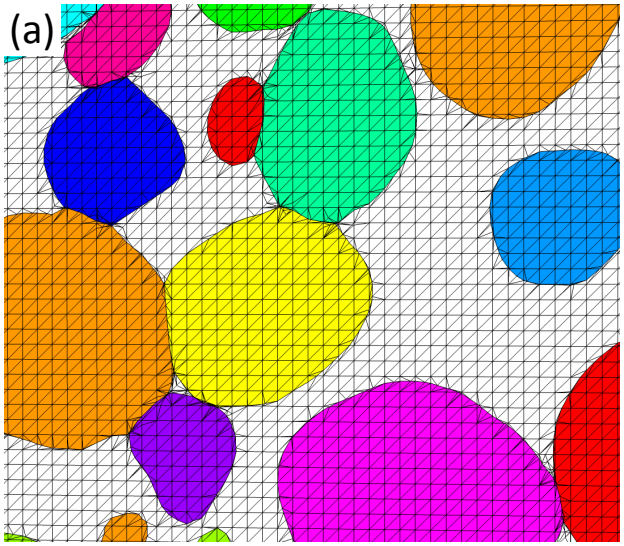

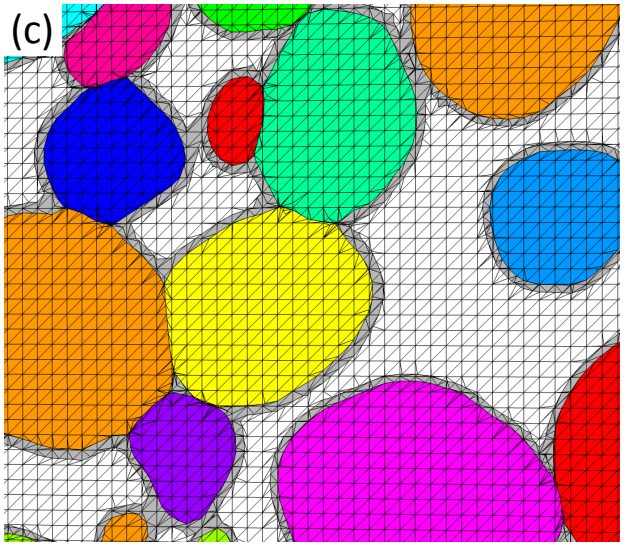

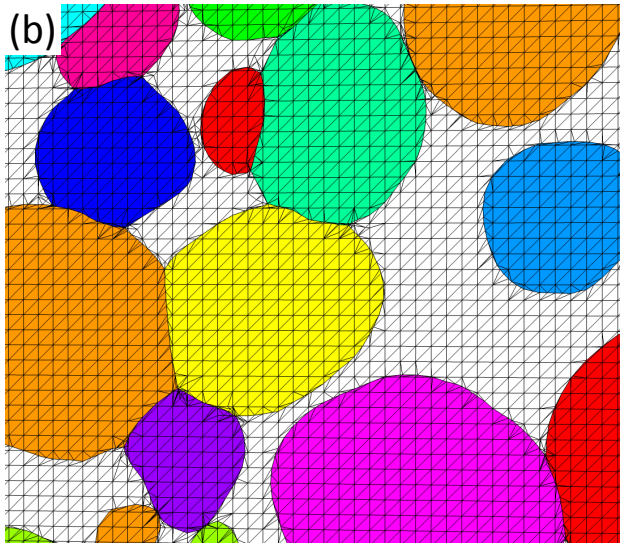

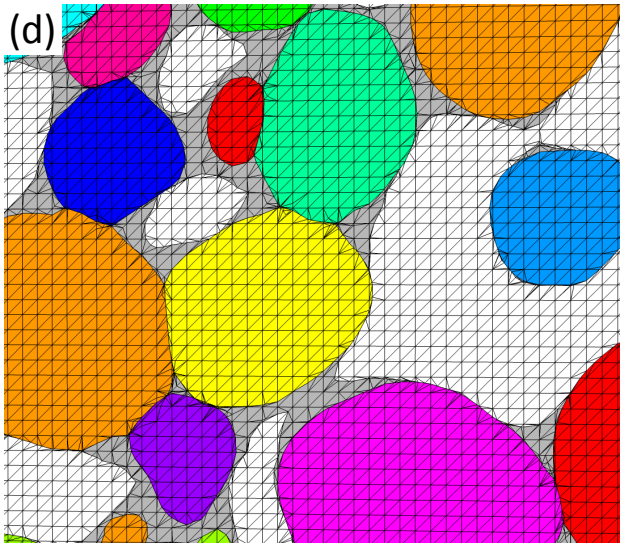

Multiple binder approaches:

(a) Raw: No binder, just particles

(b) Expanded: Expand particles to give correct porosity

(c) Coating: Coat particles with uniform binder layer to give correct porosity

(d) Contacts: Novel algorithm to place binder near particle contacts, giving correct porosity

New contact method gives binder morphology most similar to imaging

Modeling the active binder

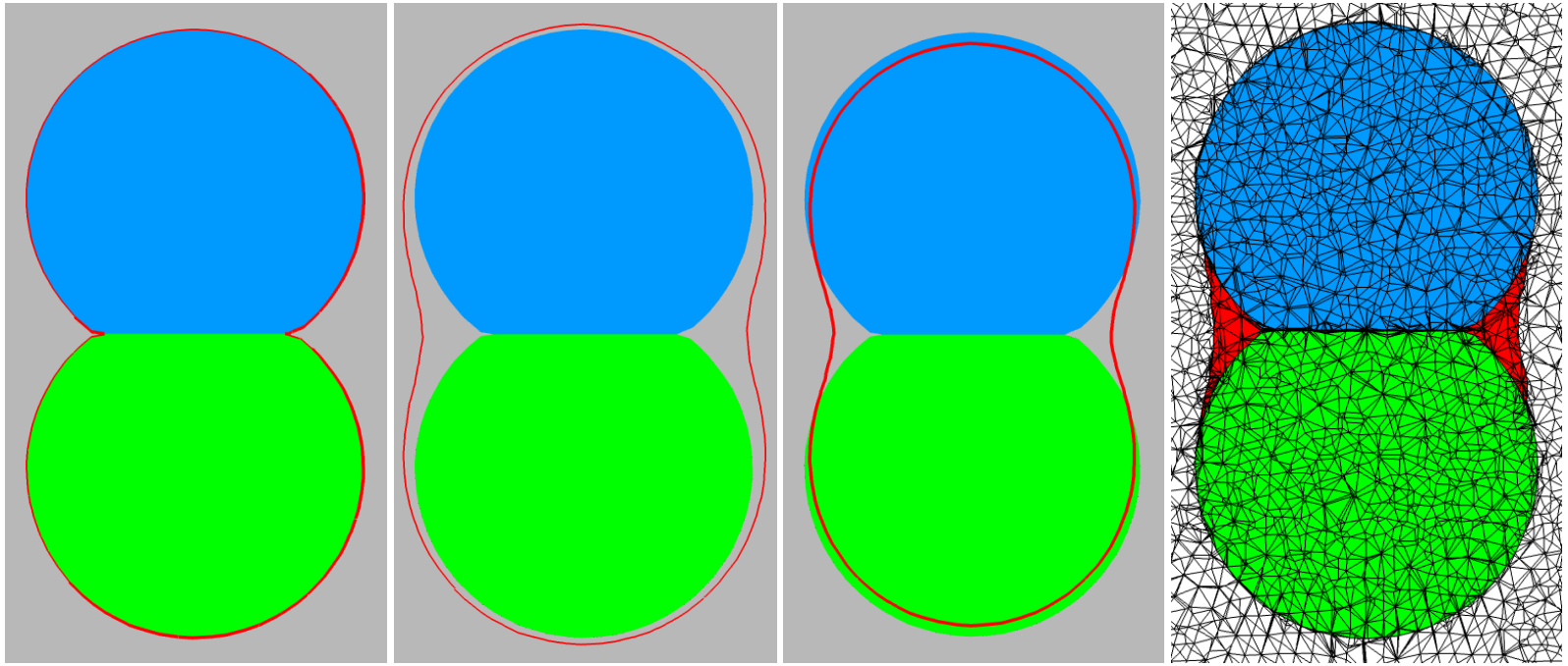

$$\phi_B = \min[(\phi_{\{p,i\}} + O)(\phi_{\{p,j\}} + O) - S, \ldots, (\phi_{\{p,N\}} + O)(\phi_{\{p,N\}} + O) - S, i \neq j$$

- Visualization of the effect of parameters O and S on two synthetic particles.
- Overlaid red line represents
  - *a)* $\phi_1\phi_2 = 0$
  - *b)* $\phi_1\phi_2 - S = 0$
  - *c)* $(\phi_1 + O)(\phi_2 + O) - S = 0$
- Final result in last image

Systematic, synthetic method for creating realistic binder morphology

NMC has lithiation-dependent properties

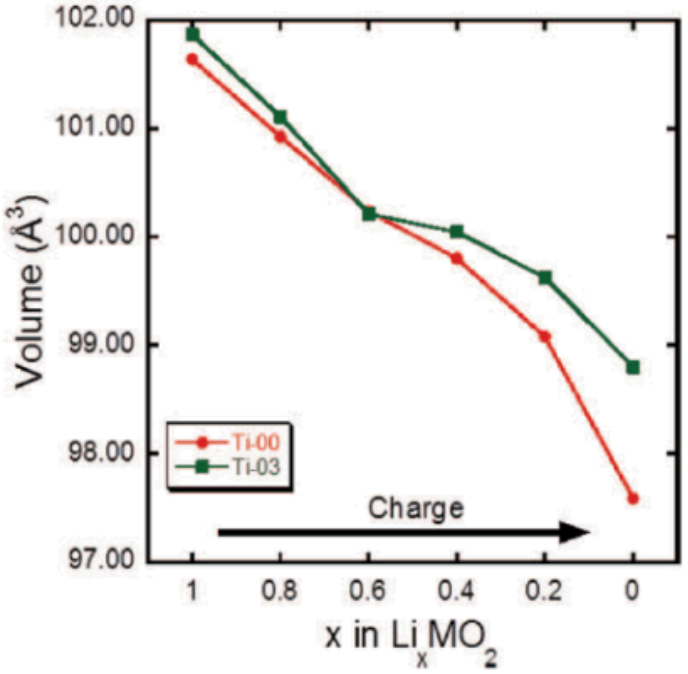

NMC particles swell as battery is discharged (Li added)

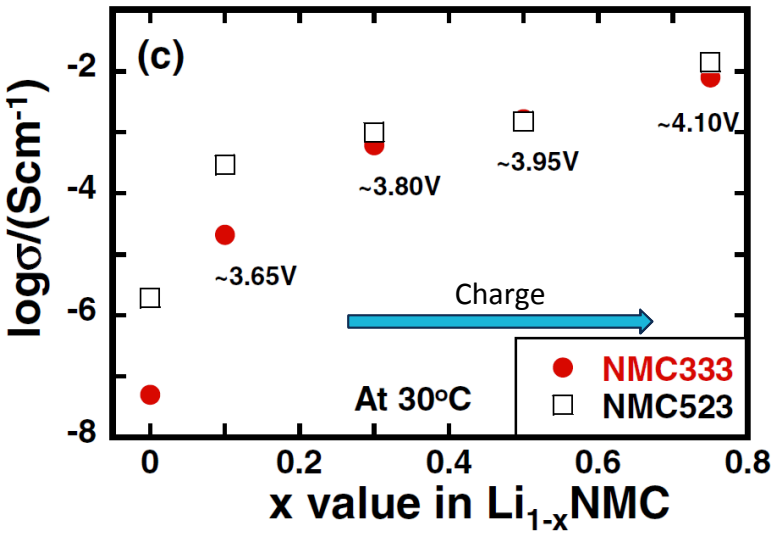

NMC electrical conductivity decreases during discharge

During discharge, conductivity decreases while swelling stresses binder

Kam (2012); Amin (2016)

Active binder has lithiation-dependent properties

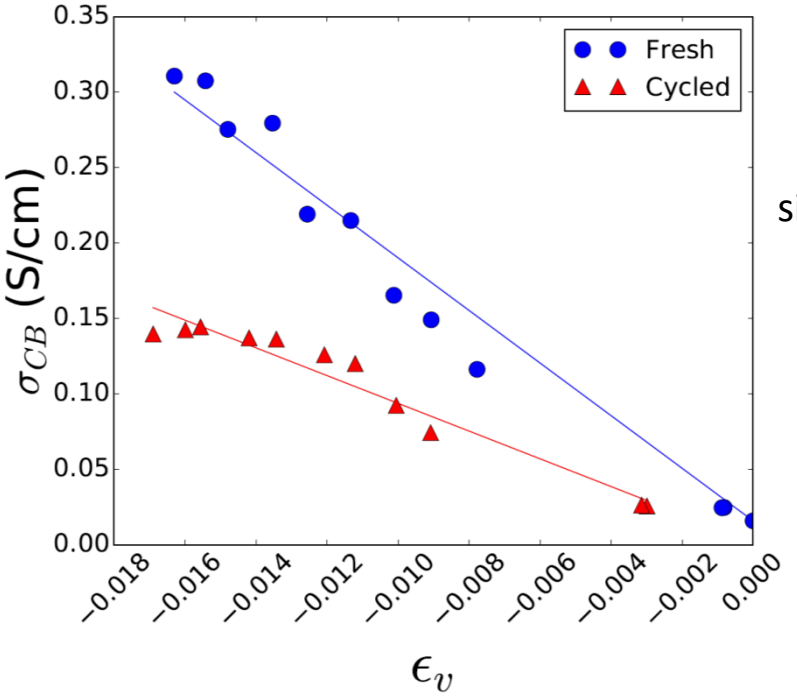

Active binder electrical conductivity increases under compression; carbon particles come into closer contact; degrades under mechanical cycling

Localized conductivity has significant impact on global conductivity; depends on morphology

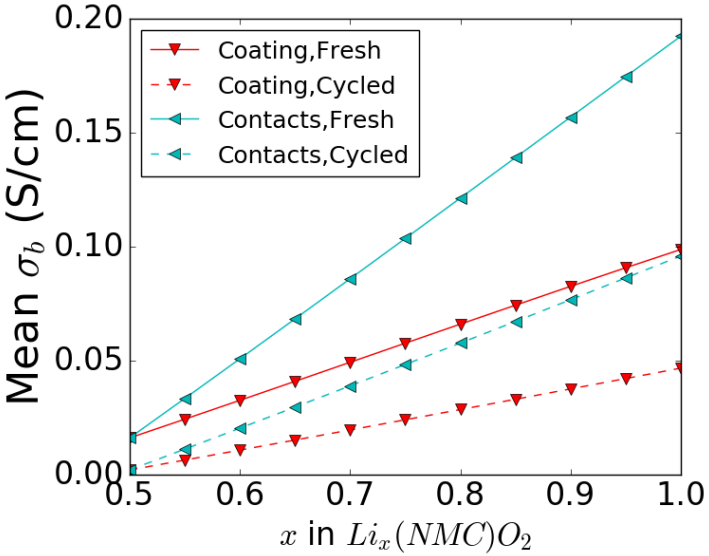

Stress localization during swelling leads to localized increase in conductivity

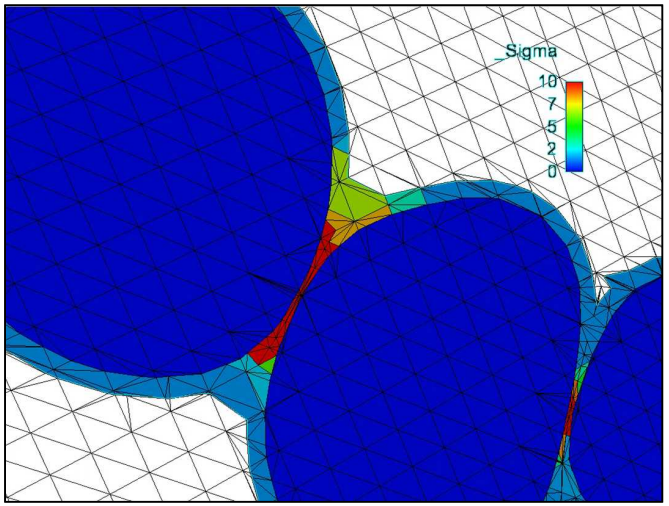

Active binder has important electro-mechanical effects

Active binder impacts: Mechanical stresses

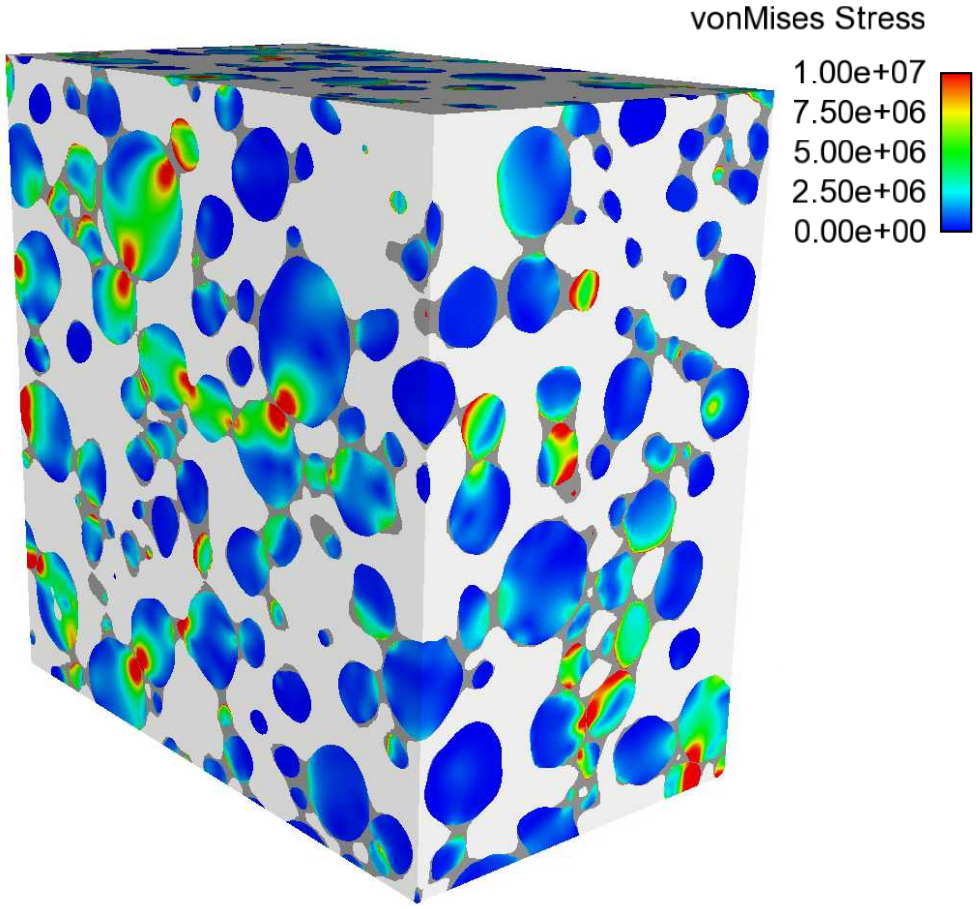

Binder undergoes compressive stress during discharge

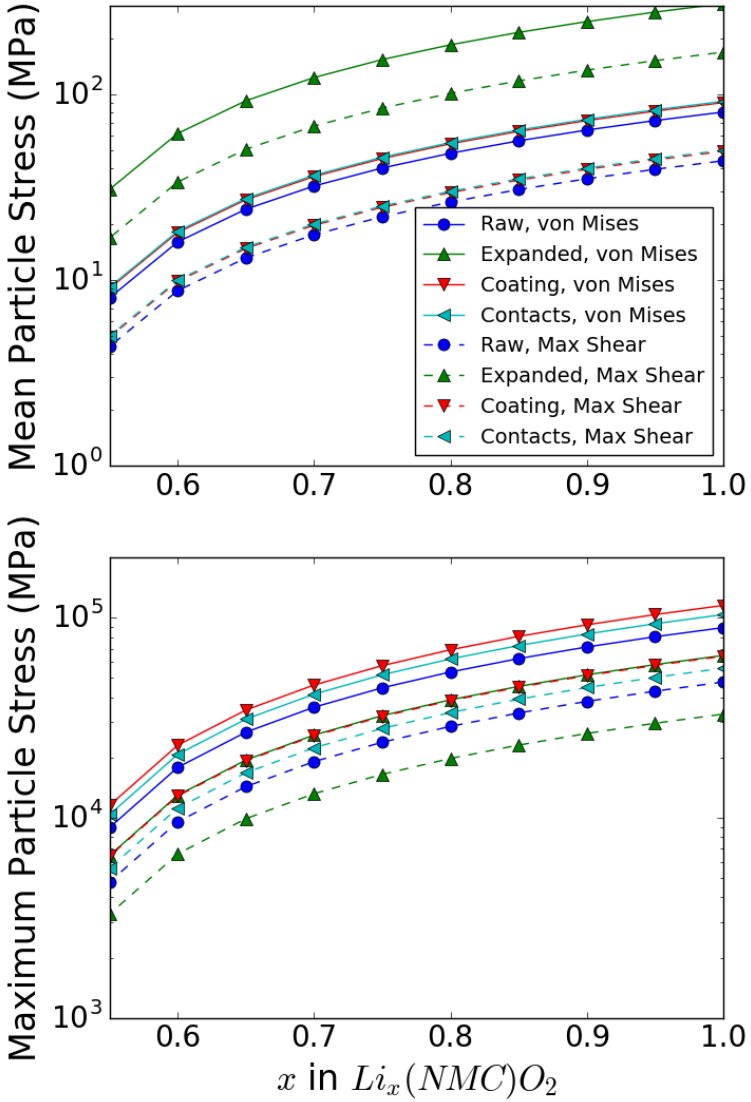

Binder significantly mitigates stress vs. hard particle contacts

Active binder impacts: Electrical conductivity

- During battery discharge
  - Lithium added (x↑)
  - NMC cond. decreases
  - Binder stress increases
  - Binder cond. increases
- Competing effects lead to nonlinear behaviors
- Aging/cycling drastically reduces conductivity
  - Harder to discharge
- Using larger binder conductivity modified tre
  for fresh batteries, less fo
  cycled

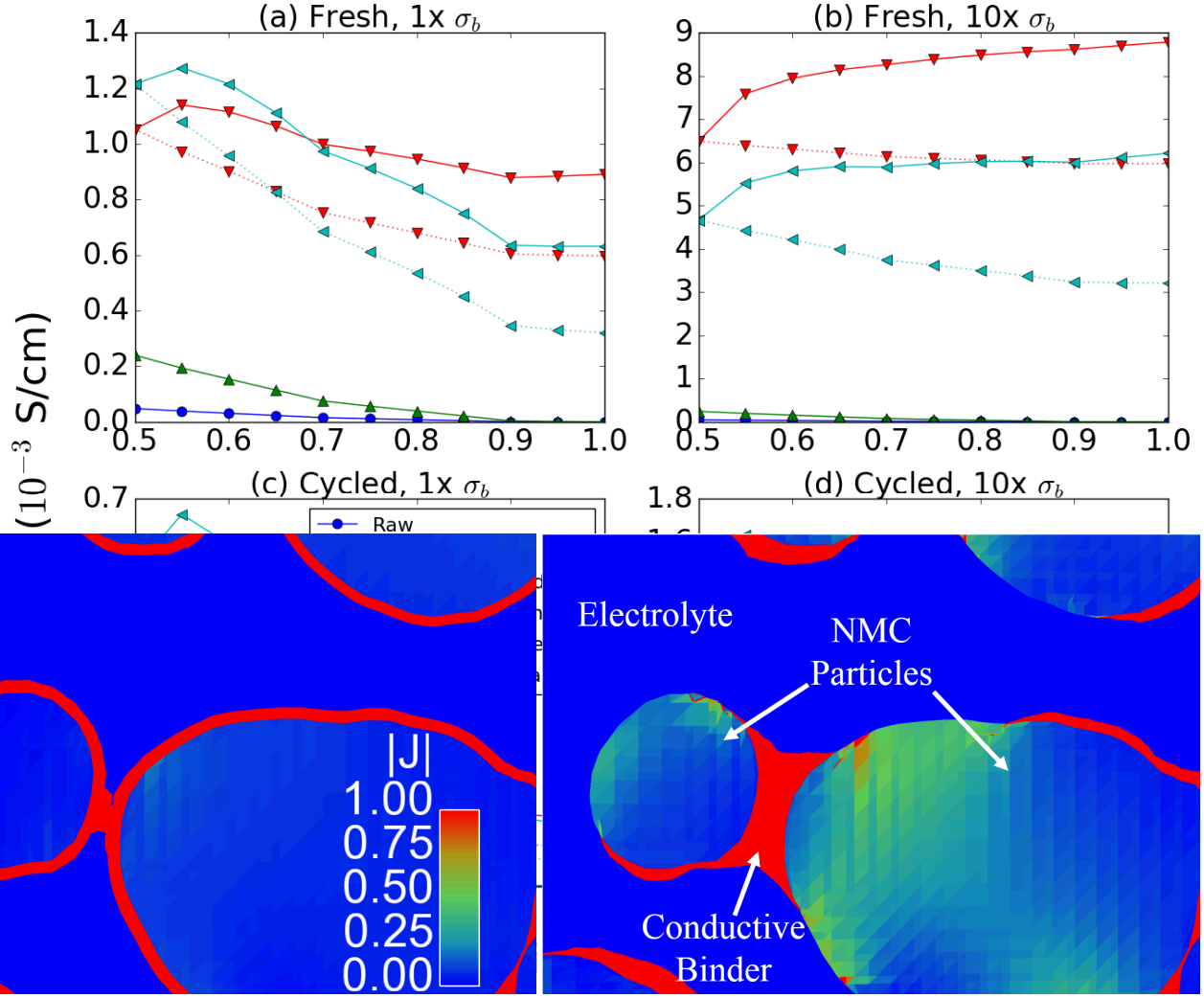

Effect of binder treatment on electrical conductivity is significant

Electrochemical mathematical model

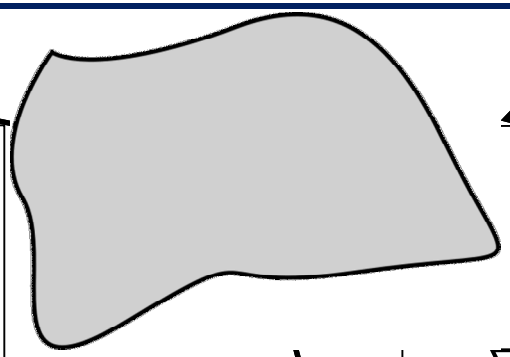

In the particle

- Ohm's Law

$$\underline{\nabla} \cdot (\sigma \underline{\nabla} \phi_{\mathrm{s}}) = 0$$

- Intercalated Li conservation

$$\frac{\partial C_{\mathrm{Li}}}{\partial t} + \underline{\nabla} \cdot \left[-M C_{\mathrm{Li}} \underline{\nabla} \left(\mu_{\mathrm{Li}}^{\mathrm{chem}} + \mu_{\mathrm{Li}}^{\mathrm{stress}} \right) \right] = 0$$

In the electrolyte

- Current conservation

$$\underline{\nabla} \cdot \left[F \left(\underline{J}_{\mathrm{Li}^+} - \underline{J}_{\mathrm{PF}_6^-} \right) \right] = 0$$

- Nernst-Planck fluxes

$$\underline{J}_i = -D_i \left(z_i C_i \frac{F}{RT} \underline{\nabla} \phi_{\mathrm{l}} + \underline{\nabla} C_i \right)$$

- Li+ conservation

$$\frac{\partial C_{\mathrm{Li}^+}}{\partial t} + \underline{\nabla} \cdot \underline{J}_{\mathrm{Li}^+} = 0$$

- Electroneutrality

$$C_{\mathrm{PF}_6^-} = C_{\mathrm{Li}^+}$$

At the interface

- Butler-Volmer reaction rate

$$\underline{J} \cdot \underline{n} = j_0 \left[\exp \left(\frac{\alpha_a F \left(\phi_{\mathrm{s}} - \phi_{\mathrm{l}} - \phi_{\mathrm{eq}} \right)}{RT} \right) - \exp \left(\frac{-\alpha_c F \left(\phi_{\mathrm{s}} - \phi_{\mathrm{l}} - \phi_{\mathrm{eq}} \right)}{RT} \right) \right]$$

Well-defined mathematical model at the mesoscale

Electrochemistry with non-ideal lithium transport - LCO

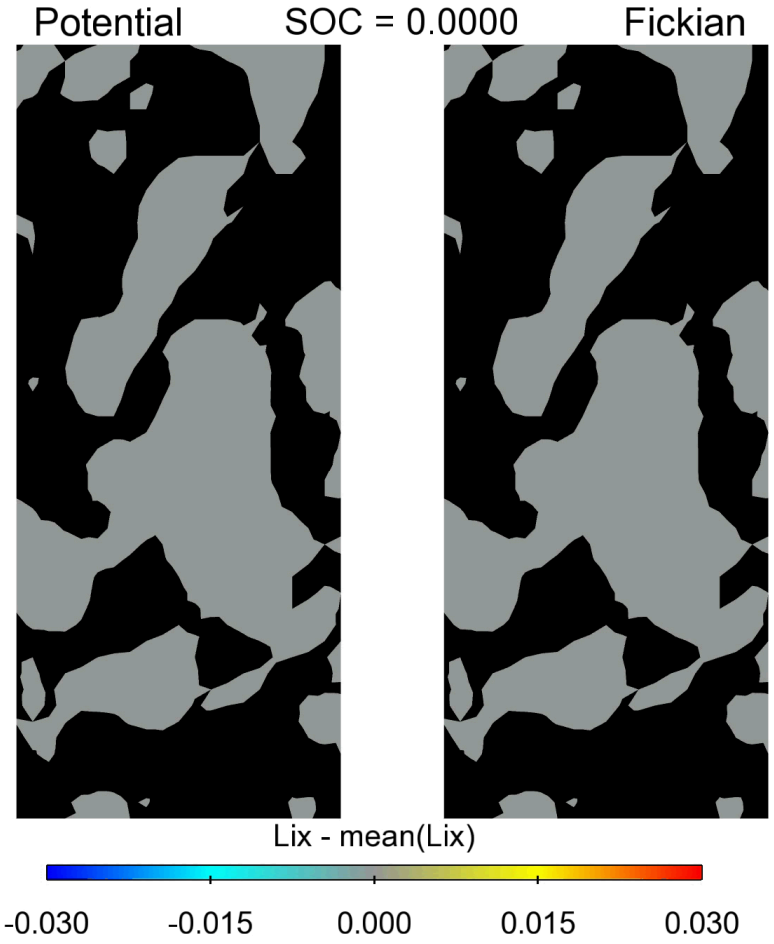

- Ideal transport (Fickian) model:

$$\underline{J}_{\mathrm{Li}} = -D\underline{\nabla} C_{\mathrm{Li}}$$

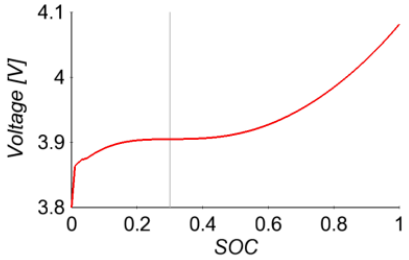

Non-ideal (potential) model:

$$\underline{J}_{\mathrm{Li}} = -MC_{\mathrm{Li}}\underline{\nabla}\mu_{\mathrm{Li}}^{\mathrm{chem}}$$

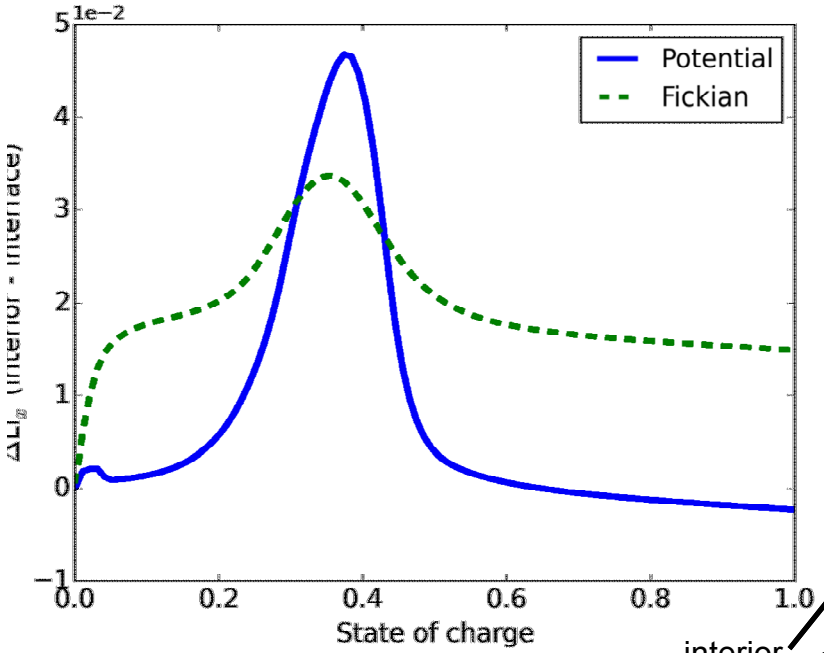

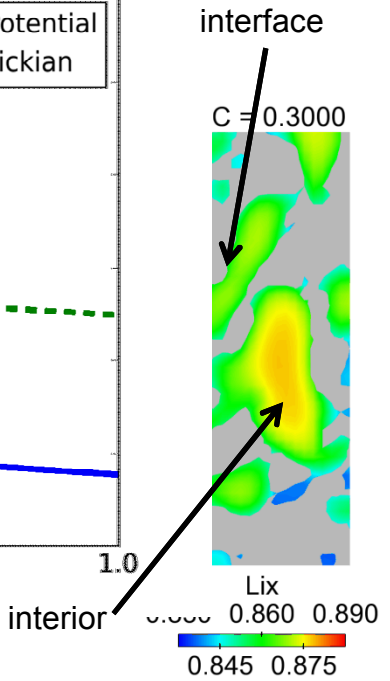

Ideal transport model shows unrealistically high concentration gradients

Mechanical mathematical model

- Intercalation-induced swelling causes a volumetric strain

$$\begin{aligned}\underline{\underline{\mathrm{E}}} &= \underline{\underline{\mathrm{E}}}_{\mathrm{elastic}} + \underline{\underline{\mathrm{E}}}_{\mathrm{swelling}} \\ &= \underline{\underline{\mathrm{E}}}_{\mathrm{elastic}} + \underline{\underline{\alpha}}\Delta C_{\mathrm{Li}}\end{aligned}$$

- For a linear elastic constitutive behavior, swelling is converted to stress
  - Analogous to standard "coefficient of thermal expansion" (e.g. Vegard's law)

$$\begin{aligned}\underline{\underline{\sigma}} &= \underline{\underline{\underline{\underline{\mathrm{C}}}}} : \underline{\underline{\mathrm{E}}}_{\mathrm{elastic}} \\ &= \underline{\underline{\underline{\underline{\mathrm{C}}}}} : \underline{\underline{\mathrm{E}}} - \underline{\underline{\underline{\underline{\mathrm{C}}}}} : \underline{\underline{\alpha}}\Delta C_{\mathrm{Li}} \\ &= \underline{\underline{\underline{\underline{\mathrm{C}}}}} : \underline{\underline{\mathrm{E}}} - \underline{\underline{\beta}}\Delta C_{\mathrm{Li}}\end{aligned}$$

- We treat volumetric strain is isotropic

$$\underline{\underline{\beta}} = \beta\underline{\underline{\delta}}$$

- Stress governed by quasi-static momentum conservation

$$\underline{\nabla} \cdot \underline{\underline{\sigma}} + \underline{F} = \underline{0}$$

Well-defined mathematical model at the mesoscale

Electrochemistry results - LCO

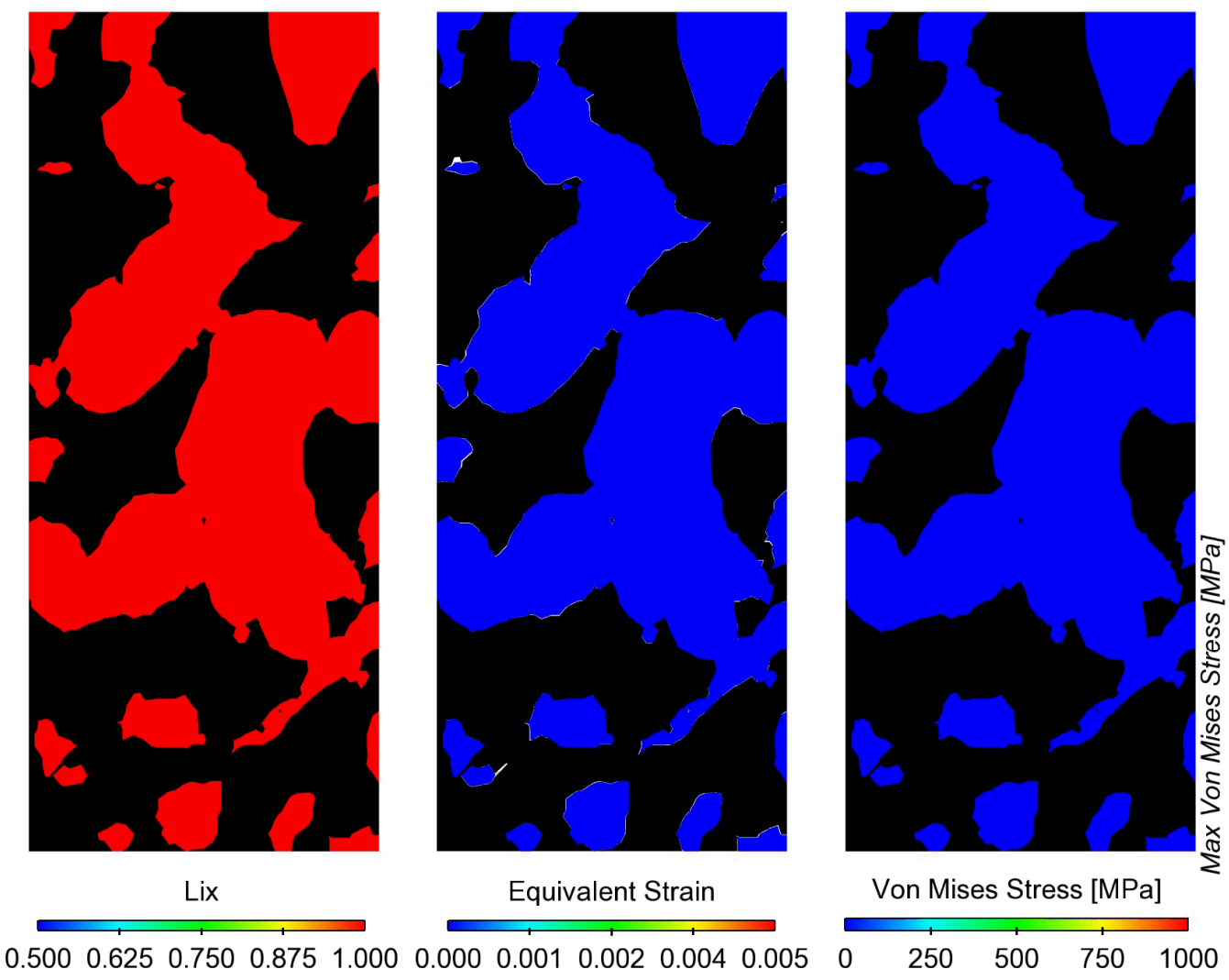

Particle confinement leads to 100x higher stress than observed in isolated particles

Electrode breathing: Effect of flexible boundaries - LCO

- Pouch cell boundary conditions can allow macroscopic swelling (breathing) while jellyrolls can be more constraining, squishing separator (Rubino et al 2001)
- Mimic this effect by controlling stiffness of upper boundary (collector)

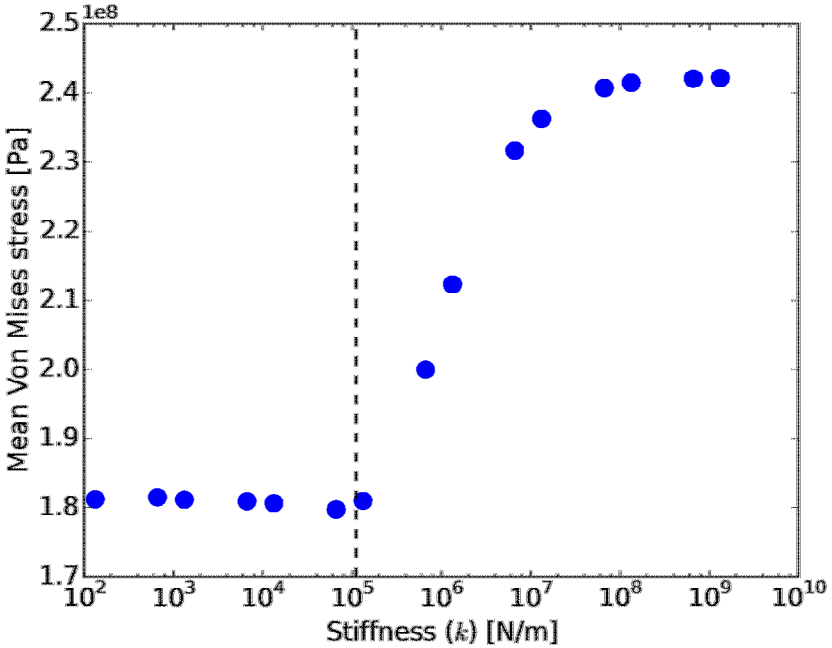

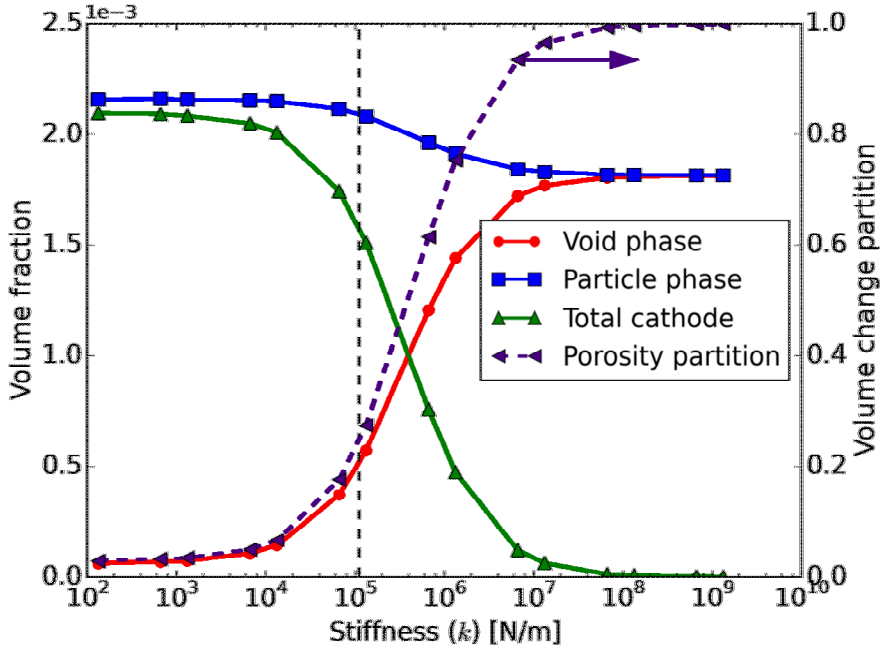

Allowing electrode breathing changes volume partitioning and reduces stress by 1/3

Mendoza et al (2016)

Summary and path forward

- Conclusions
  - Lithiation-induced swelling can lead to significant mechanical forces, degradation
  - Polymeric active binder plays a critical role in electrical transports, stress generation
  - Effective property calculations provide useful links to battery-scale models

- Future work
  - Coupled electrochemical-mechanical simulations in large NMC domains with binder
  - Upscaling results into table look-ups or curve fits for battery-scale models
  - Direct integration into battery-scale models; multi-scale approach

- Acknowledgments

  - CAEBAT-III program, DOE Vehicle Technologies Office, Brian Cunningham
  - Sandia Laboratory Directed Research and Development program
  - ORNL, LBNL, ANL, NREL, and TAMU CAEBAT-III teams for close collaboration